

# Protein kinase C iota facilitates insulin-induced glucose transport by phosphorylation of soluble nSF attachment protein receptor regulator (SNARE) double C2 domain protein b

Ryuta Nomiyama<sup>1</sup>, Masahiro Emoto<sup>1,2</sup>, Naofumi Fukuda<sup>1</sup>, Kumiko Matsui<sup>1</sup>, Manabu Kondo<sup>1</sup> , Ayuko Sakane<sup>3</sup>, Takuya Sasaki<sup>3</sup>, Yukio Tanizawa<sup>1\*</sup> 

<sup>1</sup>Division of Endocrinology, Metabolism, Hematological Sciences and Therapeutics, Yamaguchi University Graduate School of Medicine, <sup>2</sup>Emoto Clinic, Ube, and <sup>3</sup>Department of Biochemistry, Tokushima University Graduate School of Medical Sciences, Tokushima, Japan

## Keywords

Calcium sensor, Glucose transporter 4, Insulin signal

## \*Correspondence

Yukio Tanizawa  
Tel.: +81-836-22-2250  
Fax: +81-836-22-2256  
E-mail address:  
tanizawa@yamaguchi-u.ac.jp

*J Diabetes Investig* 2019; 10: 591–601

doi:10.1111/jdi.12965

## ABSTRACT

**Aims/introduction:** Double C2 domain protein b (DOC2b), one of the synaptotagmins, has been shown to translocate to the plasma membrane, and to initiate membrane-fusion processes of vesicles containing glucose transporter 4 proteins on insulin stimulation. However, the mechanism by which DOC2b is regulated remains unclear. Herein, we identified the upstream regulatory factors of DOC2b in insulin signal transduction. We also examined the role of DOC2b on systemic homeostasis using DOC2b knock-out (KO) mice.

**Materials and Methods:** We first identified DOC2b binding proteins by immunoprecipitation and mutagenesis experiments. Then, DOC2b KO mice were generated by disrupting the first exon of the DOC2b gene. In addition to the histological examination, glucose metabolism was assessed by measuring parameters on glucose/insulin tolerance tests. Insulin-stimulated glucose uptake was also measured using isolated soleus muscle and epididymal adipose tissue.

**Results:** We identified an isoform of atypical protein kinase C (protein kinase C iota) that can bind to DOC2b and phosphorylates one of the serine residues of DOC2b (S34). This phosphorylation is essential for DOC2b translocation. DOC2b KO mice showed insulin resistance and impaired oral glucose tolerance on insulin and glucose tolerance tests, respectively. Insulin-stimulated glucose uptake was impaired in isolated soleus muscle and epididymal adipose tissues from DOC2b KO mice.

**Conclusions:** We propose a novel insulin signaling mechanism by which protein kinase C iota phosphorylates DOC2b, leading to glucose transporter 4 vesicle translocation, fusion and facilitation of glucose uptake in response to insulin. The present results also showed DOC2b to play important roles in systemic glucose homeostasis.

## INTRODUCTION

In humans, glucose homeostasis is largely dependent on insulin actions<sup>1,2</sup>. This hormone stimulates the translocation of glucose transporter 4 (GLUT4) from the intracellular compartments to cell surface membranes, and enhances glucose transport into fat and muscle cells<sup>3,4</sup>. This redistribution of GLUT4 protein (GLUT4 translocation) is thought to be a key step in the

insulin action. In the past two decades, numerous studies have been carried out in an effort to reveal the molecular mechanism of insulin signaling leading to the GLUT4 translocation. Insulin activates the insulin receptor tyrosine kinase, which recruits and phosphorylates substrate adaptors, such as the insulin receptor substrate family of proteins. Tyrosine phosphorylated insulin receptor substrate binds many molecules. Among them, p85/p110-type phosphatidylinositol (PI) 3-kinase plays a major role in insulin-dependent glucose transport. Insulin receptor tyrosine

Received 25 January 2018; revised 25 September 2018; accepted 11 October 2018

kinase activity activates PI3-kinase through recruitment of SH2 domains of the p85 subunit to phosphotyrosine sites on insulin receptor substrate proteins. The 3'-phosphoinositide products of insulin-stimulated PI3-kinase are essential mediators of the insulin actions in GLUT4 translocation. Numerous studies supported a major role of these lipids in membrane trafficking.

Consequently, much effort has been expended in attempting to identify downstream targets of the PI3-kinase products that might connect insulin receptor signaling to GLUT4 glucose transporter trafficking. Many researchers have reported the possibility that the downstream targets might be factors such as Akt/protein kinase B (PKB)<sup>5-7</sup>, protein kinase C (PKC) isoforms<sup>8-10</sup>, 3-phosphoinositide 1<sup>11,12</sup> and ADP ribosylation factor proteins<sup>13</sup>. Among these molecules, recent studies have provided evidence supporting Akt/PKB and the atypical PKCs as possible downstream targets of PI3-kinase. In particular, Akt/PKB has been widely implicated as being involved in GLUT4 regulation. Other possible targets, atypical PKCs, include calcium- and diacylglycerol-independent serine/threonine protein kinases, and are involved in many cellular functions, such as cellular proliferation, migration, apoptosis, cytoskeletal regulation and glucose metabolism<sup>14,15</sup>. Among them, the PKC- $\iota$ /lambda isoform reportedly plays roles in glucose transport and glucose metabolism<sup>16-18</sup>. However, the downstream targets of atypical PKCs remain unknown.

Double C2 domain protein b (DOC2b) is a member of the synaptotagmin family of proteins that have tandem C2 domains at the C-terminus<sup>19</sup>. DOC2b has been identified as a calcium sensor protein that regulates vesicle fusion in neurons and is expressed throughout the body<sup>20,21</sup>.

Previously, we investigated the functional role of DOC2b in exocytosis in 3T3L1 adipocytes, and found that DOC2b translocated to the plasma membrane and bound to syntaxin-4 on insulin stimulation in an intracellular Ca<sup>2+</sup>-dependent manner<sup>22</sup>. This complex mediated GLUT4 vesicle fusion in 3T3L1 adipocytes. In MIN6 cells, we also found that DOC2b was necessary in the step by which insulin secretory granules fuse to the cell membrane<sup>23</sup>. These observations suggested DOC2b to be highly involved in glucose metabolism. However, it is unclear whether DOC2b is essential for whole-body glucose metabolism *in vivo*, and which signaling molecules are involved in the regulation of DOC2b.

The major aim of the present studies was to determine the precise molecular mechanism that regulates DOC2b translocation to the plasma membrane in response to insulin using 3T3L1 adipocytes. We also examined the role of DOC2b in systemic glucose homeostasis using DOC2b KO mice.

## METHODS

### Constructs and antibodies

Wild-type DOC2b was subcloned into the pGEX-6P1 vector (GE Healthcare, Buckinghamshire, UK). Munc interacting domain (MID) and mutant (S34A) were subcloned into p3 × FLAG-CMV 8.0 vector (Sigma-Aldrich, St. Louis, MO,

USA). All chemically synthesized and polymerase chain reaction-derived deoxyribonucleic acids were verified by deoxyribonucleic acid sequencing. Rabbit polyclonal DOC2b antibody was generated against the peptide sequence CGARDD-DEDVDQL. The other antibodies were commercially available and are listed in the Supplemental Methods (Appendix S1).

### Cell culture

3T3-L1 fibroblasts were grown in Dulbecco's modified Eagle's medium with 10% fetal bovine serum at 37°C. The cells (3–5 days after reaching confluence) differentiated into adipocytes with incubation in the same Dulbecco's modified Eagle's medium, containing 0.5 mmol/L isobutylmethylxanthine, 0.25 mmol/L dexamethasone and 4 µg/mL insulin, for 3 days and were then grown in Dulbecco's modified Eagle's medium with 10% fetal bovine serum for an additional 5–8 days.

### *In vitro* kinase assay

GST fusion proteins of wild-type (WT) MID, S34A MID and GST alone were purified according to the manufacturer's instructions (Promega, Madison, WI, USA). After protein concentration adjustment, these GST fusion proteins were pulled down with glutathione-sepharose beads (GE Healthcare). Precipitates were mixed with active PKC  $\iota$  (Merck Millipore, Burlington, MA, USA) and  $\gamma$ -[<sup>32</sup>P] adenosine triphosphate. After a 10-min incubation at 30°C, samples were washed with 0.75% phosphoric acid. Radioactivity was counted using an ALOKA LSC-5100 counter (Hitachi-Aloka Medical, Tokyo, Japan).

### Immunofluorescence microscopy

Differentiated 3T3-L1 adipocytes were transfected by electroporation. The cells were then re-plated onto coverslips and allowed to recover for 48 h. Cells were incubated with or without insulin for 20 min at 37°C, and then fixed with 3.7% formaldehyde in phosphate-buffered saline, permeabilized with buffer A (0.5% triton X-100, 1% fetal bovine serum in phosphate-buffered saline) for 15 min and finally incubated for 2 h with primary antibodies at room temperature. The cells were washed and incubated with an appropriate secondary antibody for 30 min. The coverslips were washed thoroughly and mounted on glass slides. Immunostained cells were observed at room temperature with a LSM 5PASCAL laser scanning confocal microscope and its two channel-scanning module (Carl Zeiss, Oberkochen, Germany) equipped with an inverted Zeiss Axiovert 200M using the 63X oil objective lens (numerical aperture 1.4) run by LSM 5 processing software (Carl Zeiss) and Adobe Photoshop CS2 (Adobe, San Jose, CA, USA).

### Generation of *Doc2* beta-deficient mice

The DOC2b KO mice were generated by replacing the DOC2b gene exon 1 with the neomycin resistance gene<sup>24</sup>. Details are given in the Supplemental Methods (Appendix S1). Male DOC2b KO mice and C57BL/6J mice, at 8–12 weeks-of-age,

were used. We maintained the DOC2b KO mice on a C57BL/6J background. Animal studies were approved by the Ethics of Animal Experimentation Committee at Yamaguchi University School of Medicine.

### Immunoprecipitation and immunoblotting

Mouse tissues (muscle, fat, isolated islets) were lysed in a lysis buffer (Thermo Fisher Scientific, Waltham, MA, USA). Cells were lysed in another lysis buffer (20 mmol/L HEPES [pH 7.2], 100 mmol/L NaCl, 1 mmol/L ethylenediaminetetraacetic acid, 25 mmol/L NaF, 1 mmol/L sodium vanadate, 1 mmol/L benzamide, 5 mg/mL leupeptin, 5 mg/mL aprotinin, 1 mmol/L phenylmethyl sulfonyl, 1 mmol/L dithiothreitol), and the protein concentrations were measured with BCA protein assay reagent (Thermo Fisher Scientific). For immunoprecipitation, the lysates were incubated with primary antibodies at 4°C for 8–12 h followed by incubation with protein-G/A-Sepharose. Lysates and immunoprecipitates were resolved by sodium dodecyl sulphate-polyacrylamide gel electrophoresis and transferred to a polyvinylidene difluoride membrane (GH Healthcare). The membranes were incubated with appropriate antibodies.

### Glucose uptake *ex-vivo* in isolated skeletal muscles and adipocytes

Mice were fasted overnight. Tissues were isolated and cut into pieces, then incubated in oxygenated incubation buffer (Krebs–

HEPES buffer with 8 mmol/L 2-deoxy-glucose, 32 mmol/L mannitol, 2 mmol/L of sodium pyruvate and 0.1% bovine serum albumin). The tissues were then stimulated with or without 100 nmol/L of insulin for 1 min, followed by the addition of 100xHOT solution (8 mmol/L 2-[<sup>3</sup>H] deoxy-glucose, 32 mmol/L [<sup>14</sup>C] mannitol) and incubation for another 20 min. After incubation, the tissues were washed with cold Krebs–HEPES buffer, then mixed with 1% Triton X-100 and boiled for 10 min. Radioactivity was counted employing an ALOKA LSC-5100 counter. The 2-[<sup>3</sup>H] deoxy glucose uptake rates were corrected for extracellular trapping using [<sup>14</sup>C] mannitol.

### Pancreas perfusion

Overnight-fasted 12–16-week-old male mice were used in perfusion experiments as described previously<sup>25</sup>. The perfusate was infused through a catheter placed in the abdominal aorta and collected from the portal vein. The perfusate was Krebs–Ringer bicarbonate HEPES buffer supplemented with 4.6% dextran and 0.25% bovine serum albumin, and bubbled with a 95% O<sub>2</sub>–5% CO<sub>2</sub> gas mixture. The flow rate of the perfusate was set at 1 mL/min. The experimental mouse pancreata were perfused with Krebs–Ringer bicarbonate HEPES buffer containing 2.8 or 16.7 mmol/L glucose. The glucose concentration was changed from 2.8 to 16.7 mmol/L at 5 min. The perfusion protocols began with a 10-min equilibration period with the same buffer

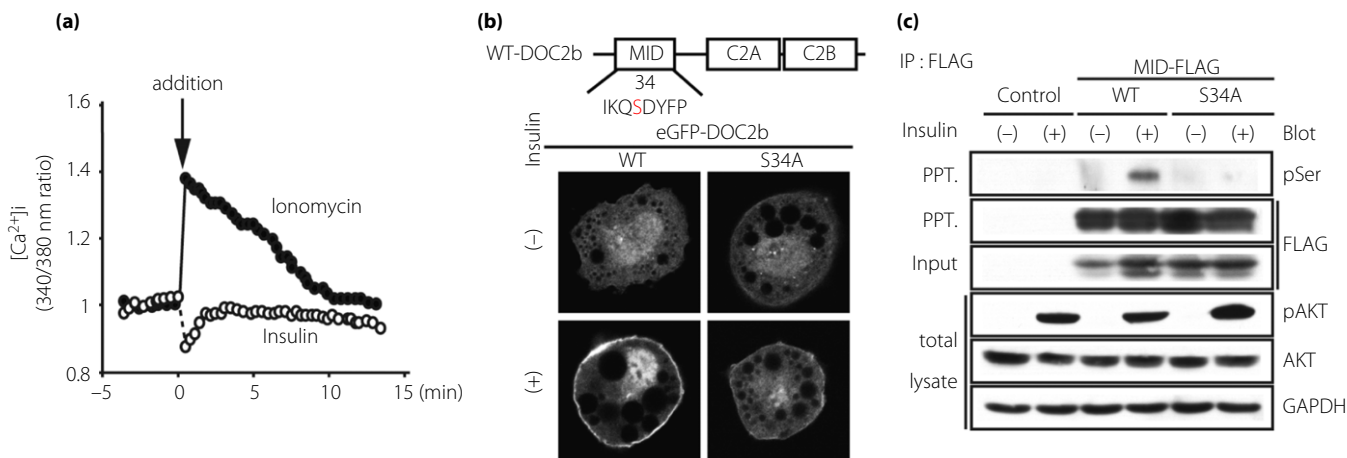


**Figure 1** | Double C2 domain protein b (DOC2b) serine 34 is phosphorylated in response to insulin stimulation. (a) 3T3L-1 adipocytes re-seeded onto glass bottom dishes were serum-starved in Krebs–HEPES buffer for 2 h at 37°C, followed by incubation with 1 μmol/L of fura-2AM for 25 min at 37°C in 10% CO<sub>2</sub>. At the end of the incubation, the cells were washed with Krebs–HEPES buffer, and a basal reading of [Ca<sup>2+</sup>]<sub>i</sub> before stimulation with either 100 nmol/L insulin or 1 μmol/L ionomycin was started. The ratio images (340 nm/380 nm excitation wavelengths) were calculated for each 3.6-s interval. (b) 3T3L-1 adipocytes were electroporated with eGFP-DOC2b (wild-type [WT] or S34A) and treated with or without 100 nmol/L insulin, and then observed by confocal microscopy. Experiments were repeated four times. Transfection efficiency was 50–60% in each experiment. At the basal condition (without insulin stimulation), very few cells had eGFP-DOC2b (both WT and S34A) green fluorescence signal on the rim of the cells. On insulin stimulation, approximately 60% of the WT DOC2b transfected cells showed rim fluorescent signal. In contrast, very few eGFP-S34A DOC2b cells had rim signal. A representative cell is shown. (c) FLAG-tagged DOC2b constructs were expressed in HEK 293 cells. After preincubation for 2 h in Krebs–HEPES buffer, the cells were treated with 1 μmol/L insulin for 7 min. Immunoprecipitation was carried out using polyclonal anti-FLAG sepharose beads. Precipitates were separated by sodium dodecyl sulphate-polyacrylamide gel electrophoresis and blotted with anti-phosphoserine antibody.

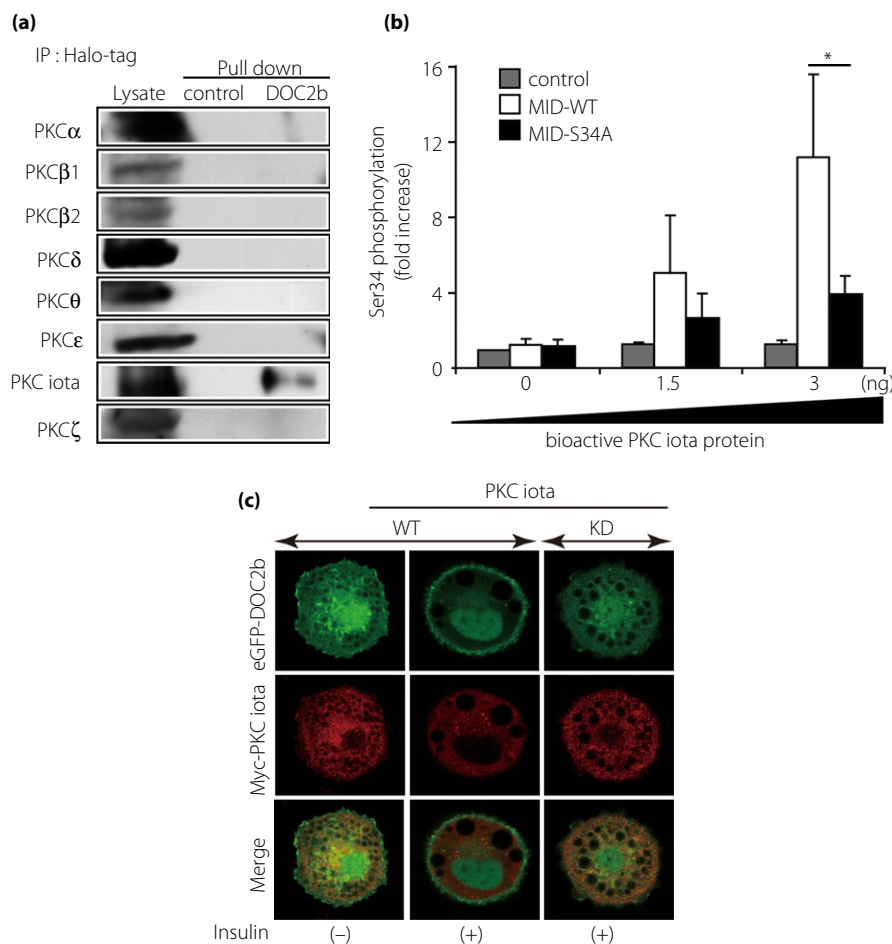


**Figure 2** | Atypical protein kinase C (PKC) iota interacts with double C2 domain protein b (DOC2b) and promotes its translocation. (a) Halo-tagged DOC2b constructs were expressed in HEK 293 cells. After preincubation for 2 h in Krebs–HEPES buffer, the cells were treated with 1  $\mu\text{mol/L}$  insulin for 10 min. Immunoprecipitation was carried out using HaloLink Magnetic Beads. Precipitates were separated by sodium dodecyl sulphate-polyacrylamide gel electrophoresis, and blotted with anti PKC $\alpha$ , PKC $\beta$ 1, PKC $\beta$ 2, PKC $\delta$ , PKC $\theta$ , PKC $\epsilon$ , PKC iota and PKC $\zeta$ . (b) GST-fusion proteins of wild-type (WT) Munc interacting domain (MID; white bar), S34A MID (black bar) and GST-alone (gray bar) were purified according to the manufacturer's instructions. After protein concentration adjustment, these GST fusion proteins were pulled down with glutathione-sepharose beads. The precipitates were mixed with PKC iota and  $\gamma$ -[ $^{32}\text{P}$ ]ATP. Radioactivity was counted with a scintillation counter. Radioactivities of each of the samples were represented as the fold-increase relative to the control without kinase. The results represent the average of three independent experiments. \* $P < 0.05$ . (c) eGFP-DOC2b and Myc-PKC iota (WT or kinase deficient mutant [KD]) were co-electroporated into 3T3-L1 adipocytes. The cells were stimulated with or without 100 nmol/L insulin for 20 min. The cells were fixed and stained with anti-Myc antibody, then observed by confocal microscopy. The experiments were repeated four times and a representative cell is shown. Transfection efficiency was 50–60% in each experiment. In the WT PKC iota co-expressed cells, DOC2b translocated to the cell membrane in approximately 60% of the transfected cells. However, when KD PKC iota was co-expressed, very few cells showed the translocation.

as that used in the initial step (i.e., from 1 to 5 min), as shown in the figures. The insulin levels in the perfusates were measured using an enzyme-linked immunosorbent assay kit (Moriyama, Yokohama, Japan).

#### Isolation of mice islets

Islets isolated from age-matched WT and DOC2b KO mice at 10–12 weeks-of-age were isolated by injection of collagenase P

(Roche Diagnostics, Mannheim, Germany) into the pancreatic duct according to standard procedures.

#### Immunofluorescent staining

Pancreata were isolated from 12-week-old mice, fixed overnight in 4% paraformaldehyde at room temperature and processed for paraffin embedding. Then, 3- $\mu\text{m}$  sections were cut and mounted on glass slides, immunostained with antibody to

insulin (Dako Cytomation, Glostrup, Denmark), and then counterstained with hematoxylin–eosin.

**Ribonucleic acid isolation and reverse transcription polymerase chain reaction**

Total ribonucleic acid (RNA) extraction was carried out with TRIzol (Invitrogen, Thermo Fisher Scientific) and the RNeasy mini kit (Qiagen, Venlo, the Netherlands) or the RNA isolation kit (Life Technologies, Thermo Fisher Scientific). Purified RNA was converted to complementary deoxyribonucleic acid with a High Capacity RNA-to-cDNA Kit (Applied Biosystems, Thermo Fisher Scientific).

All primers were designed for mouse genes. Sequences are listed in the supplemental information (Appendix S1).

**Oxygen consumption and activity amount analyses**

Oxygen consumption was measured with an O<sub>2</sub>/CO<sub>2</sub> metabolism measuring system (model MK-5000; Muromachikikai, Tokyo, Japan). Each mouse was placed in a sealed chamber (560-mL volume) with an airflow of 0.60 L/min for 24 h at 26°C. Air was sampled every 3 min, and the consumed oxygen concentration was converted to milliliters per minute by multiplying it by the flow. Oxygen consumption was normalized according to

kilogram<sup>0.75</sup> bodyweights of the mice. Activity amounts were measured using a cage with a running wheel (Model MK-700; Muromachikikai). We counted total wheel rotations for 24 h.

**Statistical analysis**

Results are expressed as the mean ± standard deviation. Differences between means were evaluated using Student’s *t* test, as appropriate. A 5% level of probability was considered to be significant.

**RESULTS**

**Serine 34 DOC2b was phosphorylated by insulin stimulations**

In cultured adipocytes, as we showed previously, DOC2b translocates from the cytoplasm compartment to the cell membrane in response to insulin stimulation, and it regulates the GLUT4 vesicle fusion process at the plasma membrane in an intracellular Ca<sup>2+</sup>-dependent manner<sup>22</sup>. However, the mechanism whereby DOC2b results in translocation to the plasma membrane remains unclear. Thus, we carried out the following experiments. Because DOC2b is a Ca<sup>2+</sup> sensor, [Ca<sup>2+</sup>]<sub>i</sub> might be elevated by insulin stimulation. However, as previously shown<sup>26</sup>, insulin did not increase [Ca<sup>2+</sup>]<sub>i</sub> in cultured adipocytes, whereas ionomycin clearly raised the [Ca<sup>2+</sup>]<sub>i</sub> (Figure 1a). We

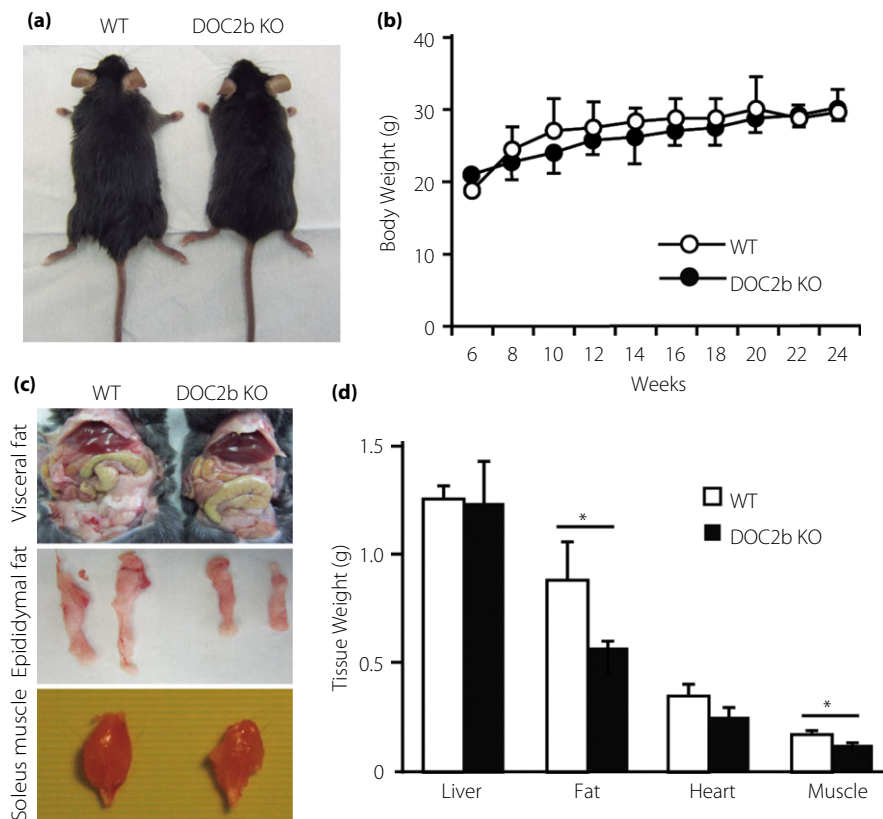


**Figure 3** | Double C2 domain protein b (DOC2b) knockout (KO) mice show impaired glucose tolerance and insulin resistance. (a) Gross appearance of wild-type (WT) mice and DOC2b KO mice. (b) Bodyweights of WT (open circle) and DOC2b KO (closed circle) mice (*n* = 6 in each group). (c) Gross images of intraperitoneal fat, epididymal fat and soleus muscle. (d) Tissue weights of the liver, heart, epididymal fat and soleus muscle from WT (white bar) and DOC2b KO mice (black bar). \**P* < 0.05.

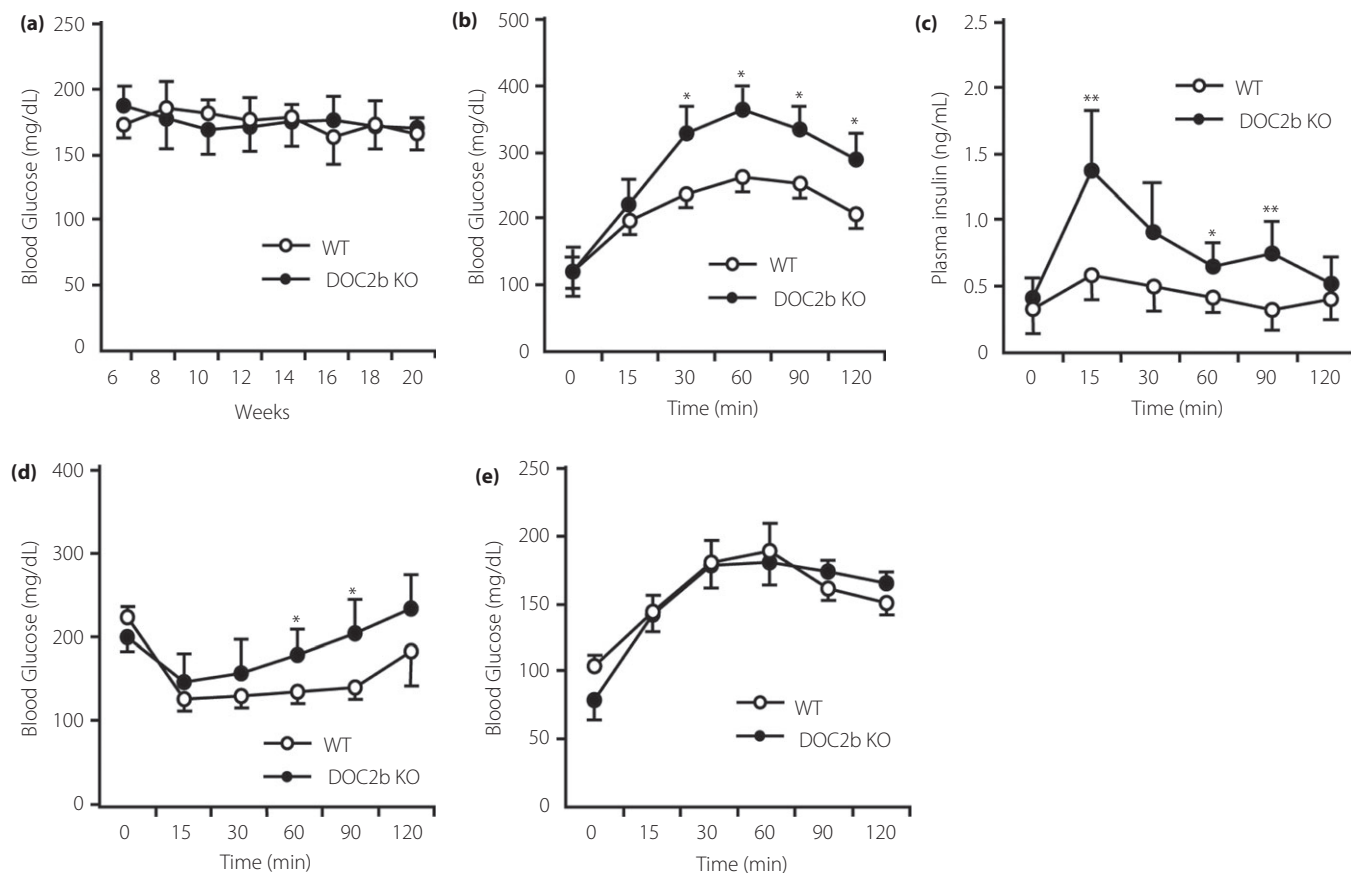


**Figure 4** | Double C2 domain protein b (DOC2b) knockout (KO) mice show impaired glucose tolerance and insulin resistance. (a) The non-fasting glucose levels of wild-type (WT; open circle) and DOC2b KO (closed circle) mice ( $n = 6$  in each group). (b–c) Glucose and (d) insulin tolerance tests in WT (open circle) and DOC2b KO (closed circle) mice at 12 weeks-of-age ( $n = 6$  in each group). (e) Pyruvate tolerance tests for WT (open circle) and DOC2b KO (closed circle) mice at 12 weeks-of-age ( $n = 6$  in each group). All results were expressed as the mean  $\pm$  standard deviation \* $P < 0.05$ , \*\* $P < 0.01$ .

previously confirmed deletion of the MID region to change intracellular DOC2b localization to the plasma membrane, even in the absence of insulin. Therefore, we hypothesized that the MID region is essential for DOC2b activation by insulin. By scanning the amino acid sequence of the MID region of DOC2b using Phospho Motif Finder<sup>27</sup>, we identified a putative serine phosphorylation motif termed “KQIS34,” presumably phosphorylated by PKC. When the serine 34 of DOC2b was altered to alanine, DOC2b failed to translocate to the plasma membrane (Figure 1b), and as shown herein, the WT serine/threonine residues in the MID region of DOC2b, but not those in the alanine 34 MID mutant, were phosphorylated on insulin stimulation (Figure 1c).

#### DOC2b was phosphorylated by atypical PKC $\iota$ , then translocated to the plasma membrane

Next, to identify the PKC isoform that phosphorylates serine/threonine residues in the MID of DOC2b, we examined each of the PKCs capable of binding to DOC2b. We found that only

atypical PKC  $\iota$  bound to DOC2b in response to insulin stimulation (Figure 2a). As atypical PKCs reportedly enhance glucose uptake in adipocytes and muscle cells<sup>10,28,29</sup>, we examined the interaction between PKC  $\iota$  and DOC2b. We also carried out an *in vitro* kinase assay to confirm that MID DOC2b could be phosphorylated by atypical PKC  $\iota$ . Atypical PKC  $\iota$  dose-dependently phosphorylated WT MID, whereas the mutant MID phosphorylation was significantly impaired (Figure 2b). Finally, we examined the role of PKC  $\iota$  in DOC2b translocation in 3T3-L1 adipocytes. Overexpression of a kinase deficient mutant PKC  $\iota$  inhibited insulin-induced translocation of DOC2b (Figure 2c). These findings indicated phosphorylation of DOC2b by PKC  $\iota$  to be essential for DOC2b translocation.

#### Impaired glucose tolerance in DOC2b KO mice

Based on the present results, we concluded DOC2b to be an insulin-signaling molecule. Therefore, we analyzed DOC2b KO mice. Neither food intake nor bodyweight differed between WT

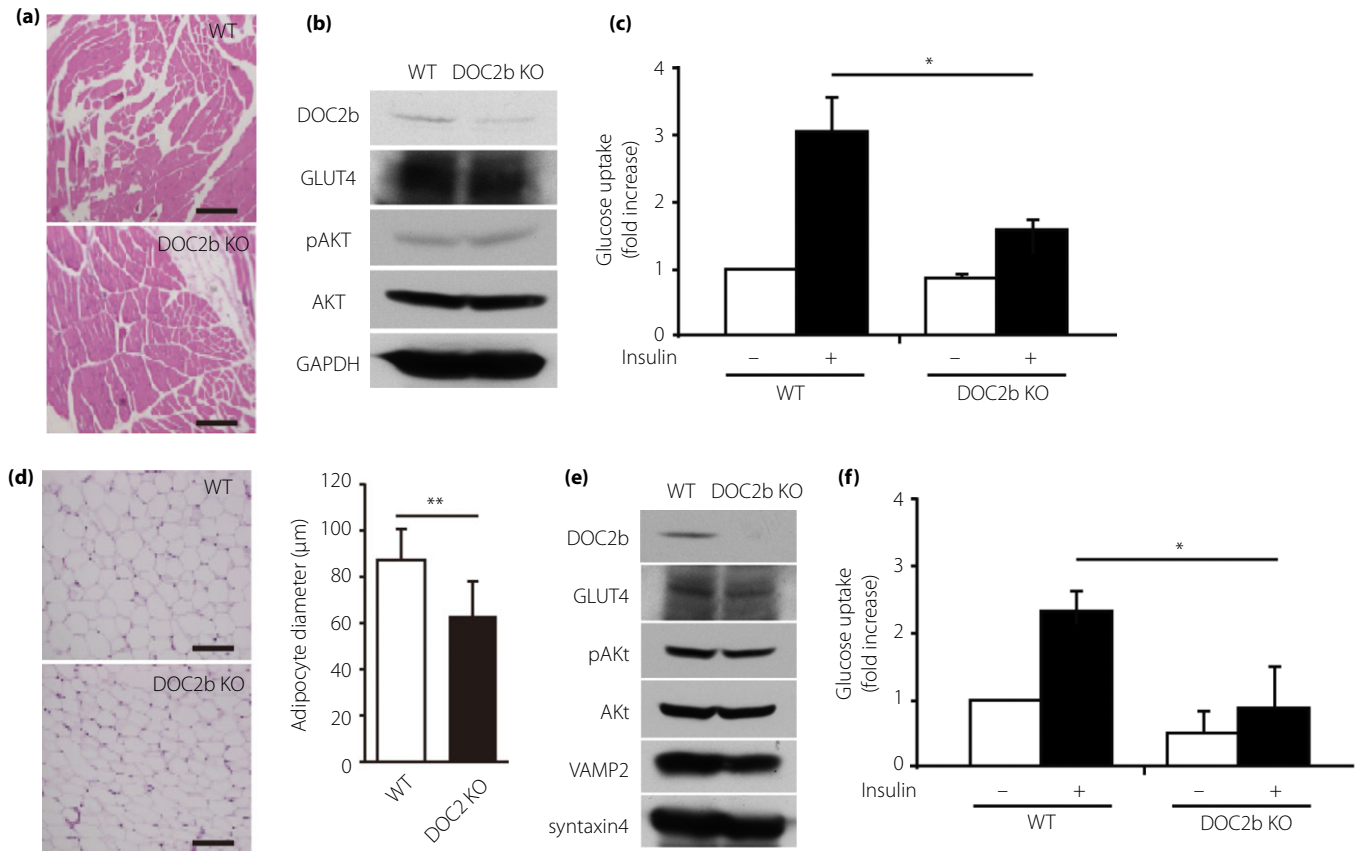


**Figure 5** | Glucose uptake in skeletal muscle and fat were reduced in double C2 domain protein b (DOC2b) knockout (KO) mice. (a) Hematoxylin-eosin staining of soleus muscle sections from wild-type (WT) and DOC2b KO mice. Scale bar, 200  $\mu$ m. (b) Immunoblotting of soleus muscle. Soleus muscle lysates were prepared from non-fasted WT and DOC2b KO mice. The cell lysates were resolved by 10% sodium dodecyl sulphate-polyacrylamide gel electrophoresis, blotted onto a polyvinylidene difluoride membrane. The membranes were incubated with primary antibodies specific for DOC2b, glucose transporter 4 (GLUT4), phosphor-AKT, pan AKT and glyceraldehyde 3-phosphate dehydrogenase (GAPDH). Data are representative of three independent sets of tissue homogenates. (c) 2-Deoxyglucose uptake in isolated soleus muscles of WT and DOC2b KO mice ( $n = 3$  in each group). (d) Hematoxylin-eosin staining of epididymal fat sections from WT and DOC2b KO mice (left). Scale bar, 200  $\mu$ m. Distribution of cell sizes in WT (white bar) and DOC2b KO (black bar) mice (right). (e) Immunoblotting of epididymal fat. Epididymal fat lysates were prepared from non-fasted WT and DOC2b KO mice. The cell lysates were resolved by 10% sodium dodecyl sulphate-polyacrylamide gel electrophoresis, blotted onto a polyvinylidene difluoride membrane. The membranes were incubated with primary antibodies specific for DOC2b, GLUT4, phospho-AKT, pan-AKT, VAMP-2 and syntaxin-4. Data are representative of three independent sets of tissue homogenates. (f) 2-Deoxyglucose uptake in isolated epididymal fat from WT and DOC2b KO mice ( $n = 3$  in each group). All results were expressed as the mean  $\pm$  standard deviation. \* $P < 0.05$ , \*\* $P < 0.01$ .

mice and DOC2b KO mice receiving a normal chow diet (Figure 3a,b). We carried out morphological observations and tissue weight measurements at 12 weeks-of-age. The epididymal fat and soleus muscle weights were significantly reduced in DOC2b KO mice, as compared with WT mice. Weights of other organs, including the heart and liver, did not differ (Figure 3c, d). We further examined glucose homeostasis in DOC2b KO mice at 12 weeks-of-age. Non-fasting blood glucose levels of DOC2b KO mice were similar to those of WT mice (Figure 4a). On glucose tolerance tests, blood glucose levels after overnight fasting were indistinguishable between the DOC2b KO mice and WT mice. The blood glucose level at 30 min

after oral glucose administration in DOC2b KO mice was significantly increased relative to that in WT mice (Figure 4b). Whereas there was no significant change in the insulin level after overnight fasting, serum insulin levels at 15, 60 and 90 min after glucose challenge were increased in DOC2b KO mice as compared with those in WT mice (Figure 4c). In insulin tolerance tests, DOC2b KO mice showed lower insulin sensitivity than WT mice (Figure 4d). In addition, we carried out the pyruvate tolerance test to evaluate glucose production from the liver, but there was no difference in the magnitude of the blood glucose increase between WT mice and DOC2b KO mice (Figure 4e). These findings suggested that DOC2b KO

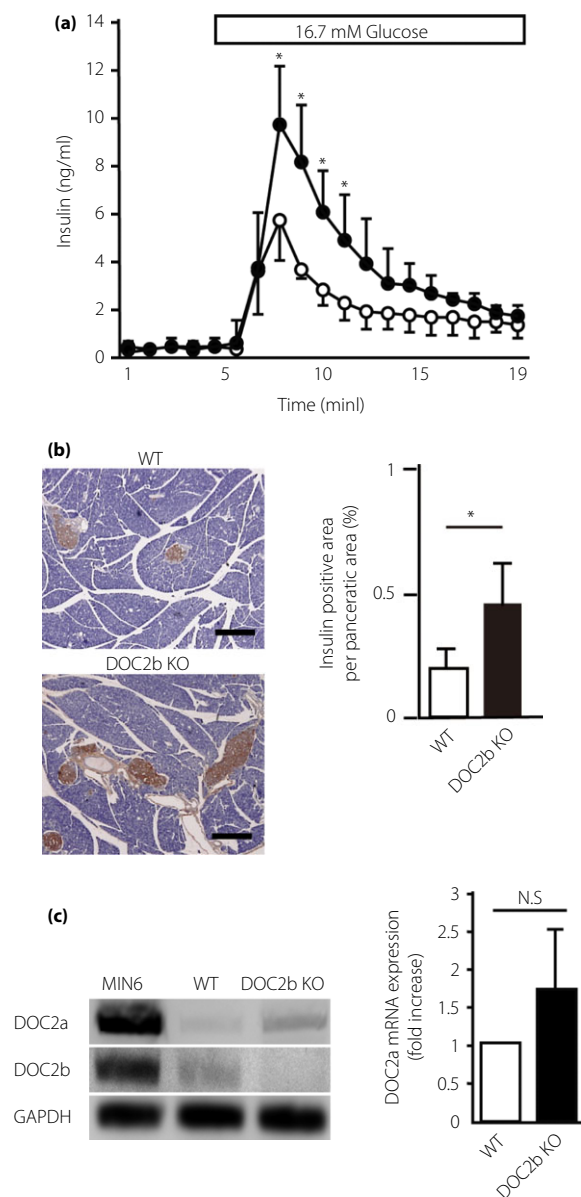


**Figure 6** | Double C2 domain protein b (DOC2b) knockout (KO) mice show enhanced insulin secretion with larger  $\beta$ -cell masses. (a) Insulin release from perfused pancreases of 12-week-old mice in response to 16.7 mmol/L glucose. Wild-type (WT) (open circle) and DOC2b KO (closed circle) mice ( $n = 4$  in each group). (b) Random pancreatic sections from 12-week-old mice with the indicated genotypes were stained with insulin antibodies and then counterstained with hematoxylin-eosin (left). Scale bar represents 300  $\mu$ m. Insulin immunoreactive cell area was expressed as the percentage of total pancreatic area (right). WT (white bar) and DOC2b KO (black bar) mice ( $n = 5$  in each group). (c) Reverse transcription polymerase chain reaction. The expressions of DOC2a in MIN6 cells, islets of WT (white bar) and DOC2b KO (black bar) mice ( $n = 4$  in each group). All results are expressed as the mean  $\pm$  standard deviation. \* $P < 0.05$ . mRNA, messenger ribonucleic acid; NS, not significant.

mice have impaired glucose tolerance and insulin resistance in muscle and adipose tissue.

#### DOC2b KO mice showed reduction of glucose uptake in insulin sensitive tissues

As impaired glucose tolerance was not caused by insulin response attenuation in DOC2b KO mice, we investigated the glucose uptake in insulin-sensitive tissues. Morphological observation of the epididymal fat in 12-week-old mice showed shrinkage of epididymal fat in DOC2b KO mice, whereas muscle histology did not differ between WT and DOC2b KO mice (Figure 5a,d). GLUT4, PKC  $\iota$ , and AKT expression levels and AKT phosphorylation in DOC2b KO mice did not differ from those in WT mice (Figure 5b,e; Figure S1). However, Insulin-stimulated glucose uptake was significantly impaired in isolated soleus muscles and epididymal fat tissues (Figure 5c,f). Thus, it was revealed that DOC2b KO mice show a reduction of glucose uptake in insulin-sensitive tissues as compared with WT mice, although the expressions of insulin signaling molecules are unaffected.

#### Enhanced glucose-stimulated insulin secretion in DOC2b KO mice

Although DOC2b KO mice show reduced glucose uptake in insulin-sensitive tissues, insulin secretion shown by the oral glucose tolerance test seemed to be enhanced. Thus, we further evaluated glucose-stimulated insulin secretion *in vivo* to determine the insulin secretory function of pancreatic islets in DOC2b KO mice. DOC2b KO mice showed significantly increased glucose-stimulated insulin secretion in perfused pancreata starting with the measurements obtained after 7 min (Figure 6a). Furthermore, pancreatic  $\beta$ -cell areas were significantly expanded in DOC2b KO mice as compared with WT mice (Figure 6b). To clarify the underlying cause, we investigated the expressions of DOC2 isoforms in the pancreatic islets by reverse transcription polymerase chain reaction. DOC2a expression appeared to show a compensatory increase in DOC2b KO mice as compared with WT mice (Figure 6c).

#### Increased energy expenditure in DOC2 KO mice

DOC2b KO mice did not differ from WT mice in daily food intake (Figure 7a). However, the amounts of activity increased (Figure 7b). Furthermore, oxygen consumption was also significantly increased in DOC2b KO mice as compared with WT mice in both the light and the dark phase (Figure 7c,d).

#### DISCUSSION

We previously showed that DOC2b promoted the membrane fusion step of GLUT4-containing vesicles to the plasma membrane in 3T3L-1 adipocytes<sup>22</sup>. Interestingly, DOC2b was rapidly translocated to the plasma membrane in response to insulin, and initiated the membrane fusion processes through its

binding to syntaxin-4 in a calcium-dependent manner. However, the precise mechanism whereby insulin regulates DOC2b has yet to be identified. As DOC2b protein is a member of the synaptotagmin family of calcium sensor proteins<sup>20</sup>, we first hypothesized that intracellular calcium might regulate DOC2b

functions. However, as shown in Figure 1a, insulin did not raise intracellular calcium concentrations, and ionomycin failed to initiate translocation of DOC2b (data not shown). These results suggest that intracellular calcium might be required for preconditioning DOC2b, and that another mechanism would be necessary for activation. We have thus developed the alternative hypothesis that DOC2b is regulated by phosphorylation at the KQIS motif in the MID domain of DOC2b. This idea was supported by the results obtained with the S34A mutant of DOC2b (Figure 1b). Taken together, the results of these and other studies have established a potential link between insulin signaling and DOC2b translocation, prompting the conclusion that DOC2b is involved in the GLUT4 vesicles membrane fusion processes in response to insulin.

A key finding of the present study is identification of PKC iota as a regulator for DOC2b. This serine/threonine kinase is one of the atypical PKC isoforms expressed in adipocytes and interacts with DOC2b, phosphorylating serine residue at the KQIS34 motif *in vivo* in response to insulin stimulation. These interesting observations were confirmed by the experiments with a kinase-dead mutant of PKC iota, as shown in Figure 2d. The present data are consistent with those of a previous report showing that atypical PKCs enhance glucose uptake in adipocytes and muscle cells<sup>10,16</sup>. Furthermore, atypical PKC iota/lambda is reportedly required for GLUT4 translocation to the plasma membrane<sup>30</sup>. Based on our or other observations, we propose a simple model whereby insulin-activated PKC iota regulates soluble N-ethyl-maleimide-sensitive fusion protein (NSF) attachment protein receptor (SNARE) regulator DOC2b, followed by interaction with syntaxin-4, initiating membrane fusion processes of GLUT4 vesicles. DOC2b might be a novel downstream effector of PKC iota, which regulates glucose transport in response to insulin.

A second significant finding reported herein is the critical role of DOC2b in whole-body glucose homeostasis. As DOC2b is known to be a SNARE regulator and facilitate glucose transport in insulin-sensitive tissues, it was expected that DOC2b deletion would cause insulin resistance in peripheral tissues/organs and would disturb glucose homeostasis. As expected,

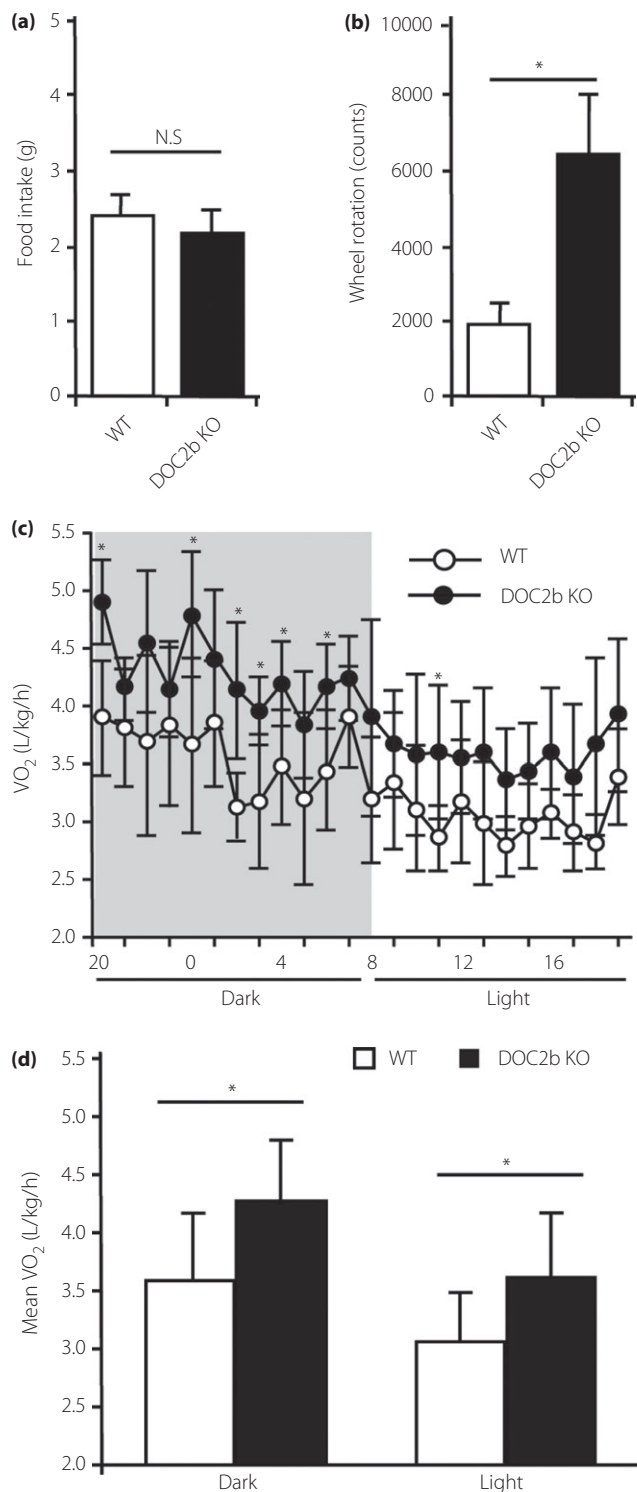


**Figure 7** | Double C2 domain protein b (DOC2b) knockout (KO) mice show increases in voluntary exercise and oxygen consumption. (a) Food intakes of wild-type (WT; white bar) and DOC2b KO (black bar) mice at the age of 12 weeks ( $n = 5$  in each group). (b) Wheel rotations were counted to record voluntary exercise during a 24 h period. WT (white bar) and DOC2b KO (black bar) mice at the age of 12 weeks ( $n = 5$  in each group). (c) The oxygen consumptions of WT (open circle) and DOC2b KO (closed circle) mice at 8–10 weeks-of-age. Measurements of oxygen consumption were carried out for 120 h, with the first day allowing the mice to acclimatize to the cage environment. The dark shadow indicates the dark phase ( $n = 5$  in each genotype). (d) Average of oxygen consumption from Figure 7c. WT (white bar) and DOC2b KO (black bar) mice. All results were expressed as the mean  $\pm$  standard deviation. \* $P < 0.05$ .

DOC2b KO mice showed impaired glucose tolerance as a result of attenuation of glucose uptake in insulin-sensitive tissue, such as muscle and fat, but not in the liver. This organ specificity might be explained by the role of DOC2b as a SNARE regulator for GLUT4-vesicular transport. In contrast, insulin action in the liver is regulated in an enzymatic manner; for example, by phosphoenolpyruvate carboxykinase activity, which is non-vesicular trafficking steps. These observations were consistent with those of previous reports<sup>31</sup>. In contrast, we observed insulin secretion to be enhanced in DOC2b KO mice, as shown in Figure 4c (glucose tolerance tests) and in Figure 6a,b (perfusion experiments and immunostaining of pancreatic specimens). These results did not appear to be consistent with our previously reported finding that silencing DOC2b impaired second-phase insulin secretion in MIN6 cells<sup>23</sup>. Taking these paradoxical observations together, we hypothesized that some compensations occurred in DOC2b KO mice. As a candidate for such mechanisms, we focused on the DOC2a isoform expressed only in pancreatic  $\beta$ -cells and neurons. As shown in Figure 6c, DOC2a expression in the pancreas appeared to be slightly increased in DOC2b KO mice, although the difference was not significant. In addition, the roles of DOC2b in insulin secretion in model mice remain controversial. One group suggested that insulin secretion was decreased in DOC2b KO mice<sup>31</sup>, whereas another noted that insulin secretion was markedly impaired in DOC2a/DOC2b double KO mice, whereas minimum effects were observed in DOC2b KO mice<sup>32</sup>. Although these controversial results have yet to be explained, the present results and those of other investigators can reasonably be taken to suggest that the effect of DOC2b loss is modest, or even minimal, and can be partly compensated by DOC2a. Furthermore, peripheral insulin resistance overwhelms these modest defects, and also leads to compensatory  $\beta$ -cell expansion, resulting in an overall increase in insulin secretion.

The observations of the effects on the central nervous system in DOC2b KO mice obtained in the present study are also interesting. DOC2b KO mice showed increased energy consumption with increasing activity. This means that DOC2b plays an additional role in the central nerve system. These observations were consistent with those of many recent studies focusing on brain science. For example, DOC2b was reported to act as a  $\text{Ca}^{2+}$  sensor protein triggering spontaneous synaptic vesicle fusion<sup>33</sup> and asynchronous exocytosis in neurons<sup>34</sup>. Interestingly, our DOC2b KO mice showed increased physical activity and oxygen consumption all day and night (Figure 7). These properties might affect the decreased adiposity in DOC2b KO mice (Figure 3c,d). In the previous report, neurotransmitter release was affected in DOC2b KO mice<sup>33,34</sup>. These observations are interesting in considering the relationship between central nerve activity and glucose metabolism.

In conclusion, the present results allow us to draw the following two conclusions. First, DOC2b plays an essential role in

systemic glucose homeostasis. Second, PKC  $\iota$  is likely to regulate DOC2b translocation and GLUT4 vesicle fusion in response to insulin. PKC  $\iota$ -DOC2b might be a novel insulin signaling mechanism that enhances glucose transport.

## ACKNOWLEDGMENTS

This work was partly supported by grants-in-aid for scientific research from Japan Society for the Promotion of Science (to ME [19659235, 24659446] and YT [18659269, 23390080, 15H04849]), and by Takeda Science Foundation (to YT). We are also very grateful to Y Kora and K Yamada for their technical support.

## DISCLOSURE

The authors declare no conflict of interest.

## REFERENCES

1. Pirola L, Johnston AM, Van Obberghen E. Modulation of insulin action. *Diabetologia* 2004; 47: 170–184.
2. Saltiel AR, Kahn CR. Insulin signaling and the regulation of glucose and lipid metabolism. *Nature* 2001; 414: 799–806.
3. Bryant NJ, Govers R, James DE. Regulated transport of the glucose transporter GLUT4. *Nat Rev Mol Cell Biol* 2002; 3: 267–277.
4. Huang S, Czech MP. The GLUT4 glucose transporter. *Cell Metab* 2007; 5: 237–252.
5. Burgering BM, Coffey PJ. Protein kinase B (c-Akt) in phosphatidylinositol-3-OH Kinase signal transduction. *Nature* 1995; 376: 599–602.
6. Cross DA, Alessi DR, Cohen P, *et al.* Inhibition of glycogen synthase kinase-3 by insulin mediated by protein kinase B. *Nature* 1995; 378: 785–789.
7. Franke TF, Yang SI, Chan TO, *et al.* The protein kinase encoded by the Akt proto-oncogene is a target of the PDGF-activated phosphatidylinositol 3-kinase. *Cell* 1995; 81: 727–736.
8. Bandyopadhyay G, Standaert ML, Zhao L, *et al.* Activation of protein kinase C ( $\alpha$ ,  $\beta$ , and  $\zeta$ ) by insulin in 3T3-L1 cells. Transfection studies suggest a role for PKC- $\zeta$  in glucose transport. *J Biol Chem* 1997; 272: 2251–2558.
9. Standaert ML, Galloway L, Kamam P, *et al.* Protein kinase C-zeta as a downstream effector of phosphatidylinositol 3-kinase during insulin stimulation in rat adipocytes. Potential role in glucose transport. *J Biol Chem* 1997; 272: 30075–30082.
10. Kotani K, Ogawa W, Matsumoto M, *et al.* Requirement of atypical protein kinase c lambda for insulin stimulation of glucose uptake but not for Akt activation in 3T3-L1 adipocytes. *Mol Cell Biol* 1998; 18: 6971–6982.
11. Klarlund JK, Guiherme A, Holik JJ, *et al.* Signaling by phosphoinositide-3,4,5-trisphosphate through proteins containing pleckstrin and Sec7 homology domains. *Science* 1997; 275: 1927–1930.

12. Li J, Malaby AW, Famulok M, *et al.* Grp1 plays a key role in linking insulin signaling to Glut4 recycling. *Dev Cell* 2012; 22: 1286–1298.
13. Fuss B, Becker T, Zinke I, *et al.* The cytohesin Steppke is essential for insulin signaling in *Drosophila*. *Nature* 2006; 444: 945–948.
14. Musashi M, Ota S, Shiroshita N. The role of protein kinase C isoforms in cell proliferation and apoptosis. *Int J Hematol* 2000; 72: 12–19.
15. Uberall F, Hellbert K, Kampfer S, *et al.* Evidence that atypical protein kinase C-lambda and atypical protein kinase C-zeta participate in Res-mediated reorganization of the F-actin cytoskeleton. *J Cell Biol* 1999; 144: 413–425.
16. Farese RV, Sajan MP, Yang H, *et al.* Muscle-specific knockout of PKC-lambda impairs glucose transport and induces metabolic and diabetic syndromes. *J Clin Invest* 2007; 117: 2289–2301.
17. Bandyopadhyay G, Standaert ML, Sajan MP, *et al.* Protein kinase C-lambda knockout in embryonic stem cells and adipocytes impairs insulin-stimulated glucose transport. *Mol Endocrinol* 2004; 18: 373–383.
18. Sajan MP, Jurzak MJ, Samuels VT, *et al.* Impairment of insulin-stimulated glucose transport and ERK activation by adipocyte-specific knockout of PKC-λ produce a phenotype characterized by diminished adiposity and enhanced insulin suppression of hepatic gluconeogenesis. *Adipocyte* 2014; 3: 19–29.
19. Sakaguchi G, Orita S, Maeda M, *et al.* Molecular cloning of an isoform of Doc2 having two C2-like domains. *Biochem Biophys Res Commun* 1995; 217: 1053–1061.
20. Kojima T, Fukuda M, Aruga J, *et al.* Calcium-dependent phospholipid binding to the C2A domain of ubiquitous form of double C2 protein (Doc2 beta). *J Biochem* 1996; 120: 671–676.
21. Groffen AJ, Brain EC, Dudok JJ, *et al.* Ca<sup>2+</sup>-induced recruitment of the secretory vesicle protein DOC2B to the target membrane. *J Biol Chem* 2004; 279: 23740–23747.
22. Fukuda N, Emoto M, Nakamori Y, *et al.* DOC2B: a novel syntaxin-4 binding protein mediating insulin-regulated GLUT4 vesicle fusion in adipocytes. *Diabetes* 2009; 58: 377–384.
23. Miyazaki M, Emoto M, Fukuda N, *et al.* DOC2b is a SNARE regulator of glucose stimulated delayed insulin secretion. *Biochem Biophys Res Commun* 2009; 384: 461–465.
24. Sakane A, Manabe S, Ishizaki H, *et al.* Rab3 GTPase-activating protein regulates synaptic transmission and plasticity through the inactivation of Rab3. *Proc Natl Acad Sci USA* 2006; 103: 10029–10034.
25. Miki T, Minami K, Shinozaki H, *et al.* Distinct effects of glucose-dependent insulinotropic polypeptide and glucagon-like peptide-1 on insulin secretion and gut motility. *Diabetes* 2005; 54: 1056–1063.
26. Kelly KL, Jude T, Corkey BE. Cytosolic free calcium in adipocytes. Distinct mechanisms of regulation and effects on insulin action. *J Biol Chem* 1989; 264: 12754–12757.
27. Peri S, Navarro JD, Amanchy R, *et al.* Development of human protein reference database as an initial platform for approaching systems biology in human. *Genome Res* 2003; 13: 2363–2371.
28. Bandyopadhyay G, Standaert ML, Galloway L, *et al.* Evidence for involvement of protein kinase C (PKC)-ζ and noninvolvement of diacylglycerol-sensitive PKCs in insulin stimulated glucose transport in L6 myotubes. *Endocrinology* 1997; 138: 4721–4731.
29. Sajan MP, Rivas J, Li P, *et al.* Repletion of atypical protein kinase C following RNA interference mediated depletion restores insulin stimulated glucose transport. *J Biol Chem* 2006; 281: 17466–17472.
30. Imamura T, Vollenweider P, Egawa K, *et al.* G alpha-q/11 protein plays a key role in insulin-induced glucose transport in 3T3L-1 adipocytes. *Mol Cell Biol* 1999; 19: 6765–6774.
31. Ramalingam L, Oh E, Yoder SM, *et al.* Doc2b is a key effector of insulin secretion and skeletal muscle insulin sensitivity. *Diabetes* 2012; 61: 2424–2432.
32. Li J, Cantley J, Burchfield JG, *et al.* DOC2 isoforms play dual roles in insulin secretion and insulin-stimulated glucose uptake. *Diabetologia* 2014; 57: 2173–2182.
33. Groffen AJ, Martense S, Diez Arazola R, *et al.* Doc2 is a high-affinity Ca<sup>2+</sup> sensor for spontaneous neurotransmitter release. *Science* 2010; 327: 1614–1618.
34. Yao J, Gaffaney JD, Kwon SE, *et al.* Doc2 is a Ca<sup>2+</sup> sensor for asynchronous neurotransmitter release. *Cell* 2011; 147: 666–677.

## SUPPORTING INFORMATION

Additional supporting information may be found online in the Supporting Information section at the end of the article.

### Appendix S1. Supplemental methods.

**Figure S1.** Protein expression of protein kinase C iota in epididymal fat.